1 May 1995

OPTICS COMMUNICATIONS

ELSEVIER

Optics Communications 116 (1995) 300–306

On the optimum spatial code of a laser anemometer

M. Saffman, T.M. Jørgensen

Department of Optics and Fluid Dynamics, Risø National Laboratory – Association EURATOM, Postbox 49, DK-4000 Roskilde, Denmark

Received 8 December 1994

Abstract

The question of the optimum spatial code of a light scattering laser anemometer is reexamined using the Fisher number as a figure of merit. We show that field distributions that are related by a Fourier transform yield the same Fisher number. The well known differential Doppler and time-of-flight configurations are therefore equally good. Comparison with a diffraction limited upper bound on the Fisher number shows that these configurations are both suboptimal. We point out that the optimum code is likely to be Fourier self-reciprocal, and show that a self-reciprocal hybrid combination of the Doppler and time-of-flight configuration yields a spatial code that is superior to those used previously.

Laser Doppler anemometry is a standard method for nonintrusive measurement of particle, surface and volume motion [1]. A variety of configurations are possible for the anemometer. In all cases there are several generic parts: transmitting optics, receiving optics and an electronic processor. The transmitting optics prepares a particular distribution of laser light in the measurement volume. The receiving optics collects the scattered light that is due to the motion of the scattering object through the measurement volume. The scattered light is detected and converted to an electronic signal for processing. The combined transmitting and receiving optics determines the spatial encoding of the signal. We address here the question of what the spatial code defined by the transmitting and receiving optics should be, such that the scattered light provides the maximum possible information about the velocity. Despite the fact that the laser Doppler anemometer is a well established and accurate measuring device this is not a purely academic question. For example, measurements of sparsely seeded high speed flows in large wind tunnels require continuous wave visible lasers with output powers in the tens of watts for accurate measurements. High powers are needed because of the combination of large measuring distances giving low collected light levels, and small seeding particles to follow accurately the high velocities. An improved spatial code would result in the same measurement accuracy with lower power lasers.

The two configurations used most often are shown in Fig. 1. In the Doppler configuration [2–4] (Fig. 1a) the differential frequency shift of light scattered quasi-elastically from a small particle passing through a pair of crossed laser beams is used to infer the magnitude of the particle velocity. In the time-of-flight configuration [5,6] (Fig. 1b) the transit time for the particle to travel between the two spots is used to infer the velocity. As is shown pictorially in Fig. 2 these two configurations are complementary; the field distributions are related by a spatial Fourier transform. Earlier investigations [7,8] that used the Fisher number [9] as a figure of merit suggested that the time-of-flight configuration is generally superior to the Doppler configuration. The analysis presented below leads to a

SSDI 0030-4018(95)00114-X

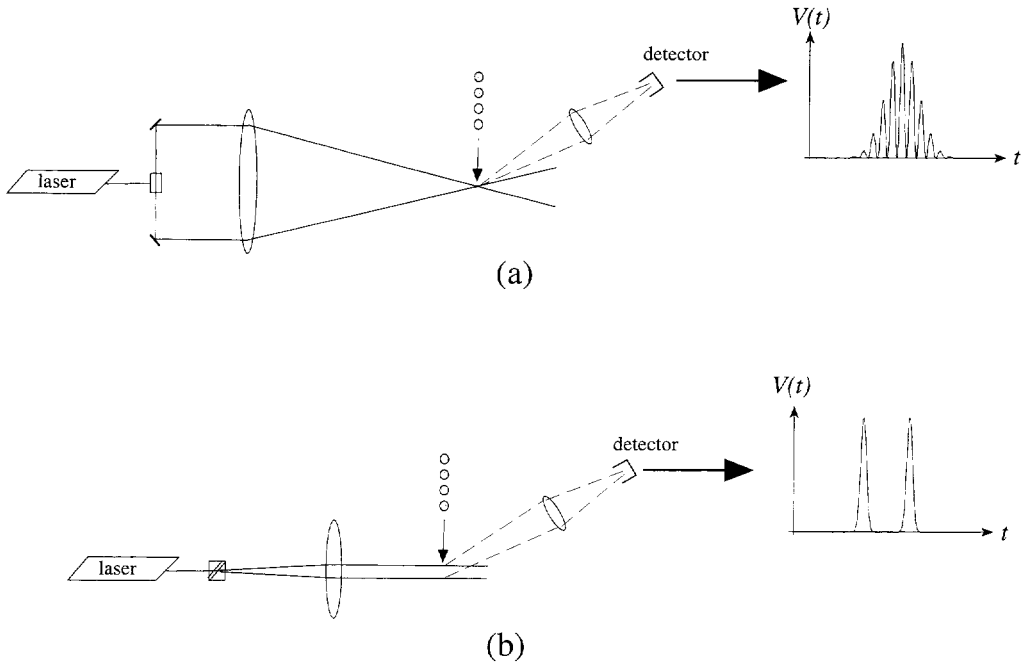

Fig. 1. Generic laser anemometer configurations: (a) Doppler and (b) time-of-flight. Idealized signals due to the passage of a single particle through the measurement region are shown for each configuration.

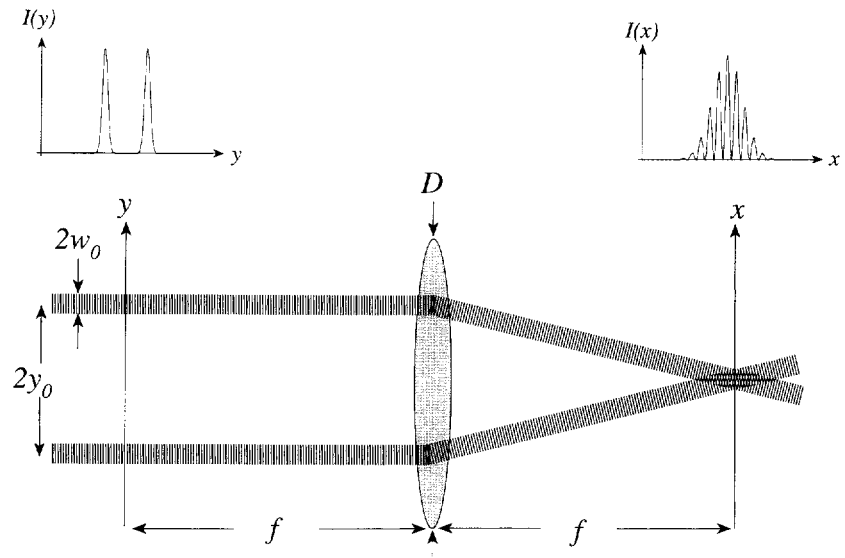

Fig. 2. The time-of-flight code in plane y is related to the Doppler code in plane x by a spatial Fourier transform.

different conclusion. We show that field distributions related by a spatial Fourier transform yield the same Fisher number. The Doppler and time-of-flight configurations are thus, in general, equivalent. However, when asymmetric constraints are imposed on the measurement system, and the finite extent of the trans-

mitting lens is accounted for, one of the configurations may be more suitable than the other. We show that when the spatial extent of the measurement volume is much less than that of the transmitting optics, as is generally the case, the Doppler configuration is slightly better. In addition, we point out that given a transmitting lens of diameter D, there is a diffraction limited upper bound on the Fisher number that scales as D^4. Both the Doppler and time-of-flight configurations yield a Fisher number that is 32 times less than the upper bound. We show that a hybrid combination of the Doppler and time-of-flight codes that is equal to its own Fourier transform [10] is superior.

The model of the anemometer assumes a single particle moving along the x axis in Fig. 2 with constant velocity v. The scattered light results in n_i photoelectron counts at time interval $\{t_i, t_{i+1}\}$. The sequence $\{n_i\}$ is assumed Poisson distributed with $p(n_i) = \bar{n}_i^{n_i} \exp(-\bar{n}_i)/n_i!$, where $\bar{n}_i = \langle n_i \rangle$ is the expected value of n_i. Assuming direct detection of the scattered light and no background signal the expected count values depend on the one-dimensional light intensity distribution $I(x)$ through $\bar{n}_i = \sigma I(x_i)\Delta t = \sigma I(vt_i)\Delta t$, where σ is the particles' scattering cross section in meters and the intensity has units of Hertz/meter. The partical trajectory is assumed to be deterministic. The statistical nature of the expected signal is due solely to the quantum photon noise.

It has been shown [7,8] that the spatial code may be optimized by using the Fisher number $F = -\langle \partial^2 \ln p(\{n_i\}|v)/\partial v^2 \rangle$ as a figure of merit. Maximizing the Fisher number minimizes the uncertainty in the estimated velocity. This follows from the fact that the lower bound on the variance of an unbiased velocity estimate is given by $\mathrm{var}[\hat{v}] = F^{-1}$, where $\hat{v}$ is the estimated velocity. Although the Fisher number may not be the simplest figure of merit for comparing alternative configurations, it is often better behaved than more intuitive alternatives. Consider, for example, the problem of estimating the mean of a Lorentzian distribution. The algebraic average is a poor estimator of the mean since it has a variance that diverges [8]. This does not imply, however, that the mean of a Lorentzian cannot be measured. In particular the Fisher number corresponding to the lower bound on the variance of an optimal unbiased estimate of the mean is finite. The point is that ad hoc estimators (e.g. the algebraic average of a Lorentzian) may have limited value, whereas the Fisher number tells us how much information it is in principle possible to extract about a given parameter, when the optimum estimator is employed. Thus the Fisher number is useful for comparing alternative approaches to parameter estimation. What the Fisher number does not do, is tell us how to find the optimal estimator. This topic is treated in depth in e.g. Ref. [11].

A straightforward calculation for the laser anemometer gives [8]

$$F = \frac{4\sigma}{v^3}\frac{1}{4}\int_{-\infty}^{\infty} \mathrm{d}x \frac{x^2}{I(x)}\left(\frac{\mathrm{d}I(x)}{\mathrm{d}x}\right)^2. \tag{1}$$

Eq. (1) is derived assuming the count numbers at different time intervals are statistically independent such that $p(\{n_i\}|v) = \prod_i p(n_i|v)$, and that the counting intervals are short compared to any dynamical time scales so that the sum may be replaced by an integral. In what follows we set the constant multiplicative factor $4\sigma/v^3$ to 1. The optimum spatial code $I(x) = |A(x)|^2$, where A is the optical field, maximizes F subject to a set of constraints. Referring to Fig. 2 we impose the following constraints:

$$P = \int_{-\infty}^{\infty} \mathrm{d}x\, |A(x)|^2, \tag{2}$$

$$\rho_x^2 = \frac{1}{P}\int_{-\infty}^{\infty} \mathrm{d}x\, x^2 |A(x)|^2, \tag{3}$$

and

$$\rho_y^2 = \frac{1}{P}\int_{-\infty}^{\infty} \mathrm{d}y\, y^2 |\tilde{A}(y)|^2. \tag{4}$$

P is the total power, and ρ_x, ρ_y are the normalized second order moments in planes x and y, respectively. Assuming paraxial optics and that the lens in Fig. 2 is sufficiently large ($D \gg \rho_x, \rho_y$) the optical fields in planes x and y are related by a Fourier transform

$$A(x) = \frac{-\mathrm{i}}{\sqrt{\pi} w_c}\int \mathrm{d}y\, \tilde{A}(y) \exp(-\mathrm{i}2xy/w_c^2), \tag{5}$$

where the confocal spot radius is $w_c = \sqrt{\lambda f/\pi}$, λ is the wavelength, and f is the focal length of the transmitting lens in Fig. 2.

To proceed, we make several intuitively reasonable assumptions about the form of $A(x)$. We wish the uncertainty in the velocity measurement to be independent of the unknown time of arrival. This implies [8] that $A(x)$ is either symmetric or antisymmetric about $x = 0$. Furthermore, we restrict attention to field distributions that can be represented in complex form with either a spatially constant argument, or an argument that varies by a factor of π. Speckle fields that are representable in the form $A(x)\exp[i\phi(x)]$ will not be considered. In this case Eq. (1) reduces to

$$F = \int \mathrm{d}x\, x^2 \left|\frac{\mathrm{d}A(x)}{\mathrm{d}x}\right|^2. \tag{6}$$

The Fisher number of the spatial code in plane y is given by

$$\begin{aligned}\tilde{F} &= \int \mathrm{d}y\, y^2 \left|\frac{\mathrm{d}\tilde{A}(y)}{\mathrm{d}y}\right|^2 \\ &= \frac{1}{\pi w_c^2}\int \mathrm{d}y\, y^2 \left|\frac{d}{\mathrm{d}y}\int \mathrm{d}x A(x)\exp(\mathrm{i}2xy/w_c^2)\right|^2 \\ &= \frac{4}{\pi w_c^6}\iint \mathrm{d}x\,\mathrm{d}x'\, xx' A(x)A^*(x') \\ &\times \int \mathrm{d}y\, y^2 \exp(\mathrm{i}2y(x-x')/w_c^2) \\ &= -\iint \mathrm{d}x\,\mathrm{d}x'\, xx' A(x)A^*(x') \\ &\times \frac{d^2}{\mathrm{d}x^2}\delta(x-x'). \end{aligned} \tag{7}$$

Integrating by parts, and assuming that $A(x)$ is well behaved, so that the contributions arising from $x|A(x)|^2$ and $x^2A(x)dA^*(x)/\mathrm{d}x$ at $x = \pm\infty$ can be neglected, leads to

$$\tilde{F} = \int \mathrm{d}x\, x^2 \left|\frac{dA(x)}{\mathrm{d}x}\right|^2 = F. \tag{8}$$

In other words the field distributions A and $\tilde{A}$ give the same Fisher number. If, in addition, the spatial constraints are symmetric ($\rho_x = \rho_y$) there is no reason to prefer one or the other of $A(x)$ and $\tilde{A}(y)$. Thus the Doppler and time-of-flight configurations are generally equivalent.

There is an additional implication of the equivalence of F and $\tilde{F}$. Both the optimum spatial code, and its Fourier transform, maximize F. If the optimum code is unique then it must be equal to its own Fourier transform. Functions that are self-reciprocal [12,13] are thus an obvious place to search for the optimum code. We show below that a simple self-reciprocal combination of the Doppler and time-of-flight configurations is indeed superior to the previously used codes.

Before comparing alternative spatial codes in more detail it is useful to have an estimate for the maximum possible Fisher number. In the optical configuration of Fig. 2 the field is negligible for $(|x|, |y|) > D/2$. Eq. (6) then gives

$$\begin{aligned} F &\le \frac{D^2}{4}\int_{-\infty}^{\infty} \mathrm{d}x \left|\frac{\mathrm{d}A(x)}{\mathrm{d}x}\right|^2 \\ &= \frac{D^2}{w_c^4}\int_{-\infty}^{\infty} \mathrm{d}y\, y^2 |\tilde{A}(y)|^2 = \frac{PD^2}{w_c^4}\rho_y^2. \end{aligned} \tag{9}$$

Alternatively, starting with the definition of F in plane y, we find $F \le (PD^2/w_c^4)\rho_x^2$. Combining the two expressions for F gives

$$F \le \frac{PD^2}{w_c^2}\frac{\rho_x\rho_y}{w_c^2}. \tag{10}$$

We see that the upper bound on F is proportional to the product $\rho_x\rho_y/w_c^2$. This result could have been anticipated by noting that the information gain as given by the Fisher number is bounded by the available information in the spatial code which has $\rho_x\rho_y/w_c^2$ degrees of freedom.

The product $\rho_x\rho_y$ has a maximum possible value when the finite lens diameter D is accounted for. Noting that the square of the second order moment in the plane of the lens is given by $\rho_x^2 + \rho_y^2$, and requiring, somewhat arbitrarily, that the second order moment does not exceed $(D/2)^2$ we find that $\rho_x\rho_y \le D^2/8$. The absolute maximum Fisher number is thus

$$F_{\max} = \frac{PD^4}{8w_c^4} = PB^2, \tag{11}$$

where we have defined the diffraction limited space-bandwidth-product of the optical system by $B = D^2/(2\sqrt{2}w_c^2)$.

The time-of-flight or Doppler configurations are described analytically by

$$\tilde{A}(y) = \alpha\{\exp[-(y - y_0)^2/w_0^2] + \exp[-(y + y_0)^2/w_0^2]\}. \quad (12)$$

$\tilde{A}(y)$ corresponds to the field in plane y of Fig. 2, and the normalization constant α is fixed by requiring $P = 1$. $\tilde{A}(y)$ defines a Doppler configuration if plane x is assumed to be the measurement plane, and it defines a time-of-flight configuration if plane y is assumed to be the measurement plane. Using Eqs. (3), (4), (6) we find

$$F = \tfrac{3}{4} + n_f^2 \tanh(n_f^2), \quad (13)$$

$$\rho_x^2 = \frac{w_c^4}{4w_0^2}\left(1 - 4\frac{n_f^2}{1 + \exp(2n_f^2)}\right), \quad (14)$$

$$\rho_y^2 = \frac{w_0^2}{4}\left(1 + 4\frac{n_f^2}{1 + \exp(-2n_f^2)}\right), \quad (15)$$

where $n_f \equiv y_0/w_0$ is $\pi/4$ times the number of fringes between the $1/e^2$ points of the wavepacket envelope. Evaluating Eqs. (13)–(15) in the limit of $n_f \gg 1$ we find $F/(\rho_x\rho_y) \sim 2n_f/w_c^2$, which implies that n_f should be made as large as possible for optimal utilization of the available space-bandwidth product. Requiring that the $1/e^2$ intensity points of all beams are contained within $\pm D/2$ in the lens plane leads to, for $n_f \gg 1$, $n_{f,\max} \simeq D^2/16w_c^2$, which is obtained for $y_0 = D/4$ and $w_0 = 4w_c^2/D$. The diffraction limited maximum possible Fisher number is thus $F_{\max} \sim D^4/256w_c^4$, and is shown in Fig. 3 as a function of the dimensionless ratio D/w_c. By comparison, the upper bound on F given by Eq. (11) is a factor 32 larger. We conclude that the time-of-flight and Doppler configurations are suboptimal.

Although the Doppler and time-of-flight configurations lead to the same Fisher number in the presence of symmetric constraints on the second order moments the imposition of asymmetric spatial constraints may select a preferred configuration. In practice it may be desirable to measure the velocity in a small region of space, whereas the spatial constraint on the transmitting optics is equal to the lens diameter D which is typically much larger. For the Doppler configuration this implies that $\rho_x \ll \rho_y$, whereas for the time-of-flight configuration this implies $\rho_x \gg \rho_y$. The Fisher number is maximized for $n_f = n_{f,\max}$ in which case, using the values of w_0 and y_0 from the preceeding paragraph, $\rho_x/\rho_y = 0.5$. For a given value of $n_f < n_{f,\max}$ the minimum possible value of ρ_x/ρ_y is less than the inverse of the maximum possible value of ρ_x/ρ_y. In other words, when the constraint is to have a well localized measurement volume, a slightly higher Fisher number can be achieved, for a fixed lens diameter, using a Doppler configuration. However, the difference between the two configurations is not large, and typically other considerations, such as the expected velocity distribution and the choice of signal processing, will dictate which configuration is preferable.

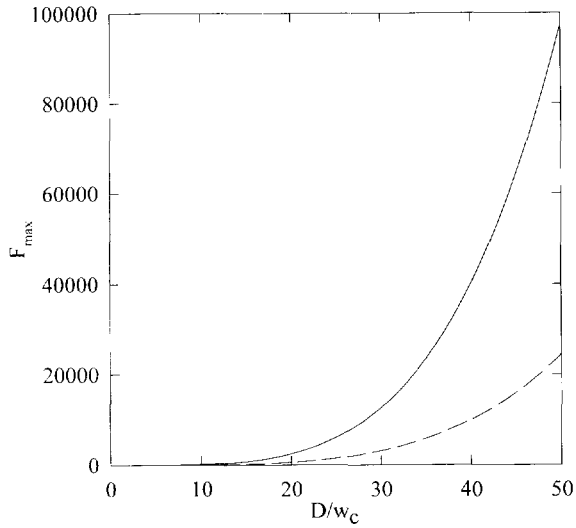

Fig. 3. Diffraction limited maximum Fisher number for the hybrid (solid line) and Doppler/time-of-flight (dashed line) codes as a function of the ratio D/w_c.

The question remains as to which spatial code yields the maximum Fisher number given by Eq. (11)? A single Gaussian beam, which is described by letting $y_0 \to 0$ in the expression for $\tilde{A}(y)$, is not as good as the time-of-flight or Doppler configurations. A more general field consisting of N Gaussians spaced uniformly in the interval $-y_0 < y < y_0$ is worse than the two beam configuration for any N greater than 2. In the limits of $N \gg 1$ and $n_f \gg 1$ the Fisher number grows proportional to n_f^2 but at a rate 3 times slower than that given by Eq. (13). It appears that a two beam code is in some sense optimal. Looking at Eq. (6) it is tempting to keep two widely spaced beams, but to increase the value of dA/dx by modulating the field under each Gaussian envelope. We are thus led to the hybrid configuration, shown in Fig. 4, and defined analytically by

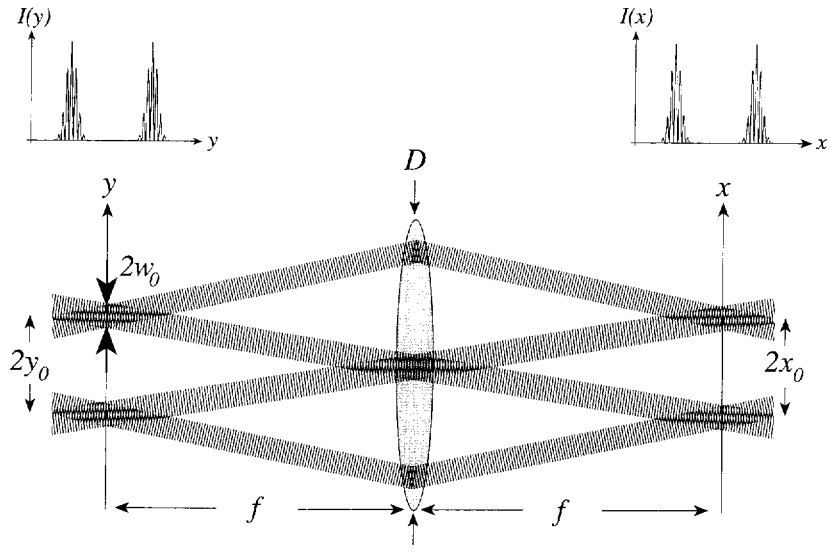

Fig. 4. Hybrid combination of the Doppler and time-of-flight configurations.

$$\tilde{A}(y) = \alpha\left[\exp\left(-\frac{(y-y_0)^2}{w_0^2}\right)\cos\left(\frac{x_0(2y-y_0)}{w_c^2}\right) + \exp\left(-\frac{(y+y_0)^2}{w_0^2}\right)\cos\left(\frac{x_0(2y+y_0)}{w_c^2}\right)\right], \tag{16}$$

where α is a normalization constant. This type of configuration was proposed recently [10], as an approach to improving the spatial resolution of measurements of density fluctuations in plasmas. The signals from this type of anemometer can be processed in a variety of ways to estimate the velocity. An approach based on envelope detection of each of the Doppler bursts, followed by cross-correlation of the bursts, has been described in Ref. [10]. Envelope detection has the advantage of making the velocity estimate insensitive to the relative phase of the two Doppler bursts.

Analysis shows that, given a finite lens diameter D, the Fisher number is maximized by the symmetric configuration described by $x_0 = y_0$ and $w_0 = w_c$. Eqs. (3), (4), (6) then give

$$F = \frac{3}{4} + \frac{2n_f^2 a + 4n_f^4[1+\exp(4n_f^2)]}{b}, \tag{17}$$

$$\rho_x^2 = \rho_y^2 = \frac{w_c^2}{4} + w_c^2 n_f^2 \frac{a}{b}, \tag{18}$$

where

$$a = \exp(4n_f^2) - 2\sin(2n_f^2)\exp(2n_f^2) - 1,$$

$$b = \exp(4n_f^2) + 2\cos(2n_f^2)\exp(2n_f^2) + 1.$$

For small n_f the detailed behavior of F on n_f depends on the choice of phases in the arguments of the cosines in Eq. (16). The form used here was chosen to make (16) self-reciprocal, such that the phase of the sinusoidal modulation with respect to the peaks of the Gaussians is the same in both planes x and y. For $n_f \gg 1$, $F/(\rho_x\rho_y) \sim 4n_f^2/w_c^2$, and is independent of the choice of phase. Requiring again that the $1/e^2$ intensity points of all beams are contained within $\pm D/2$ in the lens plane leads to, for $n_f \gg 1$, $n_{f,\max} \simeq D/(4w_c)$, and $F_{\max} \sim D^4/64w_c^4$, as shown in Fig. 3. Note that the hybrid configuration has a Fisher number that is 4 times larger than that of the Doppler or time-of-flight systems, for the same aperture D.

It is instructive to look at how the different spatial codes utilize the available aperture in the lens plane. Fresnel propagating the fields defined by Eqs. (12), (16) to the plane of the lens leads to the intensity distributions shown in Fig. 5. The integrated intensity in the two curves is equal. The hybrid code is more effective at localizing a larger fraction of the energy further from the optical axis. This results in a larger Fisher number for the same available lens aperture. The remaining factor of 8 separating the Fisher number of the hybrid code from the theoretical maximum given

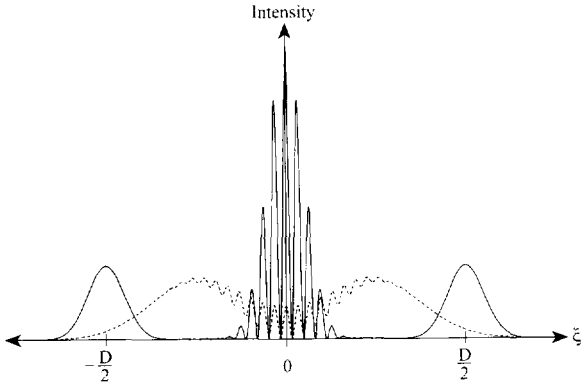

Fig. 5. Intensity distributions versus spatial coordinate ξ in the plane of the lens for hybrid (solid line) and Doppler/time-of-flight (dashed line) configurations. For the hybrid configuration $n_f = D/(4w_c)$ giving $F = 600$, and for the Doppler/time-of-flight configuration $n_f = D^2/(16w_c^2)$ giving $F = 150$. The intensity of the hybrid code at $\xi = \pm D/2$ is down by a factor of about $2/e^2$ compared with the intensity at $\xi = 0$. As the value of D/w_c is increased the ratio approaches $1/e^2$. For pictorial clarity the value $D/w_c = 14$ was used for both curves.

by Eq. (11) is to some degree arbitrary. If we require instead that the second order moment in the lens plane is at most $D^2/4$, we find that the hybrid code achieves the theoretical maximum Fisher number, although the Doppler/time-of-flight is still suboptimal. In this case, however, the intensity peaks of the hybrid code centered at $\xi = \pm D/2$ in Fig. 5, lie fully outside the lens aperture. The point is that the second order moment can be insensitive to intensity components lying far from the optical axis, whereas in a real optical system there is always a finite available aperture.

In summary we have shown that the Doppler and time-of-flight laser anemometers are in general equivalent, and both suboptimal. A self-reciprocal hybrid combination leads to a spatial code that utilizes the available space-bandwidth product more effectively. It should be emphasized that the present analysis is restricted to the case of single particles with no background noise. Allowing for multiple particles and background noise may lead to different conclusions than those presented here.

References

[1] L.E. Drain, The laser Doppler technique (Wiley, 1980).
[2] C.M. Penney, IEEE J. Quantum Electron. 5 (1969) 318.
[3] H.D. vom Stein and H.J. Pfeifer, Metrologia 5 (1969) 59.
[4] B.S. Rinkevichyus, Radio Eng. Electron. Phys. (USSR) 14 (1969) 1648.
[5] R. Schodl, in: AGARD Conf. Proc. No. 193 (Saint-Louis, France, 1976) p. 21-1.
[6] L. Lading, in: AGARD Conf. Proc. No. 193 (Saint-Louis, France, 1976) p. 23-1.
[7] A. Skov Jensen and L. Lading, The optimum code in single-particle velocity estimation with a laser anemometer, Risø-R-413 (Risø National Laboratory, Roskilde, Denmark, 1980).
[8] L. Lading and T.M. Jørgensen, J. Opt. Soc. Am. A 7 (1990) 1324.
[9] R.A. Fisher, Proc. Cambridge Philos. Soc. 22 (1925) 700.
[10] L. Lading, M. Saffman, S.G. Hanson, and R.V. Edwards, A Combined Doppler and Time-of-Flight Laser Anemometer for Measurement of Density Fluctuations in Plasmas, J. Atmos. Terr. Phys. (1995) to appear.
[11] H.L. Van Trees, Detection, Estimation and Modulation Theory (Wiley, New York, 1968) Part I.
[12] E.C. Titchmarsh, Introduction to the Theory of Fourier Integrals, 2nd edition, (Oxford U. Press, Oxford, 1948).
[13] M.J. Caola, J. Phys. A 24 (1991) L1143.